CHEMISTRY JOURNAL OF MOLDOVA. General, Industrial and Ecological Chemistry. 2022, 17(2), 73-83
ISSN (p) 1857-1727 ISSN (e) 2345-1688
http://cjm.ichem.md
http://dx.doi.org/10.19261/cjm.2022.957

SYNTHESIS, CHARACTERIZATION AND ANTIBACTERIAL ACTIVITY OF FERROCENE LIGANDS AND THEIR BINUCLEAR COMPLEXES

Ozan Süleyman Ürgüt [a*], Aydin Tavman [b], Muazzez Gürgan Eser [c]

[a]*Department of Chemistry, Faculty of Arts and Sciences, Tekirdag Namik Kemal University, Namik Kemal District, Degirmenalti Campus, 1, Campus str., Suleymanpasa-Tekirdag 59030, Turkey*
[b] *Department of Chemistry, Engineering Faculty, Istanbul University-Cerrahpasa, University District, 7, Baglarici str., Avcilar-Istanbul 34320, Turkey*
[c]*Department of Biology, Faculty of Arts and Sciences, Tekirdag Namik Kemal University, Namik Kemal District, Degirmenalti Campus, 1, Campus str., Suleymanpasa-Tekirdag 59030, Turkey*
[*]*e-mail: ourgut@nku.edu.tr, phone: (+90 282) 25 026 52*

Abstract. 6-Chloro-2-ferrocenyl-1*H*-benzimidazole and (*E*)-((4-chloro-2-hydroxyphenylimino) methyl)ferrocene ligands and their Fe(III), Co(II), Cu(II), Zn(II) and Pd(II) complexes were synthesized. The structures of compounds were confirmed on the basis of elemental analysis, FT-IR, ^{1}H and ^{13}C NMR, UV-Vis spectroscopy and mass spectrometry. In addition, magnetic moment and molar conductivity measurements were performed for the complexes. The Fe(III), Cu(II), Zn(II) and Co(II) complexes do not manifest electrolytic properties while Pd(II) complexes have electrolytic properties. All the complexes coordinate in a 1:1 M:L ratio. Benzimidazoles have a potential to be used as antibacterial agents alternative to current antibiotics to which bacteria gain resistance day by day. The antibacterial activity of the ligands and the complexes was investigated against *Staphylococcus aureus* and *Escherichia coli*. The obtained complexes generally show considerable high activity compared to the ligands, and it was revealed that the complexes of benzimidazole presented a more pronounced activity in comparison to other investigated compounds. The high activities of the Co complex of the benzimidazole ligand and the Zn complex of the Schiff base ligand against *Staphylococcus aureus* (2 and 4 mg/mL, respectively), are noteworthy.

Keywords: azomethine, binuclear complex, organometallic, transition metal complex, antibacterial property.

Received: 23 May 2022/ Revised final: 08 August 2022/ Accepted: 11 August 2022

Introduction

Many organometallic cyclic molecules have been synthesized in recent years, especially metallocenes, which are of particular interest as they have different coordination abilities and can withstand multiple electron transfer processes. Ferrocene is one of the most popular metallocene complex. Ferrocene derivatives have received great interest due to their potential applications as sensitive electrochemical sensors, nonlinear optical materials, antibacterial and anticancer drugs, nanotube materials, catalysts, ionic recognition and redox fluorescent switch [1,2]. There has been great interest in the functionalization of metallocene molecules; addition of ferrocene to some coordination compounds increases their cytotoxic activity. The affinity of the two cyclopentadiene rings in ferrocene to bond and the redox ability of the central iron explain this success, allowing ferrocene to be tuned to different challenges [3]. Benzimidazole is a bicyclic organic compound formed by the fusion of benzene and imidazole rings [4]. Ferrocene-based benzimidazole derivatives are attracting much attention for the synthesis of new heterocyclic complexes with many applications including ionic recognition, metal complexes, fluorescent probes, enantioselective and heterogeneous catalysts [5]. The properties that ferrocene gives to heterocyclic moiety are now of great interest to researchers [6].

Schiff bases obtained from amino and aldehyde compounds contain an azomethine group (-HC=N-), which is an important class of ligands that coordinate with metal ions through the nitrogen atom. The presence of azomethine group is important in elucidating the mechanism of biological transformation and racemization reaction [7]. Ferrocenyl bonded to Schiff base compounds creates a link between organometallic chemistry and molecular biotechnology.

Schiff base molecules have great potential sites for biochemically active compounds related to intermolecular hydrogen bonding and proton

transfer equilibrium. The transition metal complexes of some Schiff bases are of interest because of their antifungal, antibacterial and antitumor activities, as well as their spectroscopic properties and applications [8].

The aim of this study was to synthesize ferrocene derivatives of benzimidazole and Schiff base ligands structurally similar and to obtain their metal complexes, to examine and compare the structural properties and antibacterial effects of all the compounds. Thus, the 6-Chloro-2-ferrocenyl-1*H*-benzimidazole, **L1**, and (*E*)-((4-chloro-2-hydroxyphenylimino)methyl)ferrocene, **HL2**, ligands, and their Fe(III), Co(II), Cu(II), Zn(II) and Pd(II) complexes were synthesized and characterized. The antibacterial activity of the ligands and the complexes was tested against *Escherichia coli* and *Staphylococcus aureus* strains.

Experimental

Generalities

Dichloromethane (anhydrous, ≥99.8%), acetic acid (≥99.8%), ethyl alcohol, methyl alcohol (≥99.8%), acetonitrile, acetone (≥99.5%), ethyl acetate, *n*-hexane, dimethyl sulfoxide (DMSO), potassium chloride (99.0-99.5%), boric acid, ferrocenecarboxaldehyde, 2-amino-4-chlorophenol, 4-chloro-*o*-phenylenediamine, iron(III) chloride, copper(II) chloride dihydrate, cobalt(II) chloride hexahydrate, zinc(II) chloride, and palladium(II) chloride hexahydrate were purchased from Sigma-Aldrich and Supelco and used without further purification.

Elemental analysis data were obtained by using a Thermo Finnigan Flash EA 1112 analyzer.

Molar conductivity of the complexes was measured on a VWR Phenomenal conductometer CO 3000 L in dimethylformamide (DMF) at 25±1°C.

Magnetic moment measurements for the paramagnetic complexes were carried out on a Sherwood Scientific apparatus (MK1) at room temperature by Gouy's method.

FT-IR spectra were recorded on a Bruker Optics Vertex 70 spectrometer using ATR (Attenuated Total Reflection) techniques.

^{1}H NMR (500 MHz, DMSO-d_6) and *^{13}C NMR* (125 MHz, DMSO-d_6) spectra were registered on a Varian Unity Inova 500 NMR spectrometer.

The *electron spray ionization-mass spectroscopic* (ESI-MS) analyses were carried out in positive ion modes using a Thermo Finnigan LCQ Advantage MAX LC/MS/MS.

UV-Vis spectra were performed on a Shimadzu UV-2600UV-Vis Spectrometer at molar concentration of 10^{-2} in DMSO.

Synthesis

*6-Chloro-2-ferrocenyl-1H-benzimidazole (**L1**)*

The novel **L1** was synthesized according to the literature method with a minor modification [9]. To the well stirred solution of ferrocenecarboxaldehyde (0.214 g, 0.001 mol) in ethanol (10 mL) was added 0.001 mol H_3BO_3 and stirred with gentle heating for 30 minutes followed by addition of an ethanolic solution of 4-chloro-*o*-phenylenediamine (0.142 g, 0.001 mol). The reaction mixture was further refluxed with continuous stirring for 2 hours; the progress of the reaction was monitored with thin layer chromatography (TLC) upon completion of the reaction. The reaction was terminated with water and allowed to cool to room temperature, and then filtered with vacuum. The filtered claret red product was washed with ethanol. The obtained solid phase was filtered, washed with ethanol several times and dried in a vacuum drying oven, giving a clear yellow solid compound. A quantity of 0.239 g (71%) of the reaction product **L1** was obtained with m.p. 267–269°C. Anal. calcd. for $C_{17}H_{13}ClFeN_2$ (formula weight: 336.0): C, 60.66; H, 3.89; N, 8.32%; found: C, 59.87; H, 4.12; N, 8.11%. ESI-MS (*m/z*, %): 337.2 ($[M+H]^+$, 100), 199.2 (10.4). Molar conductivity Λ_M (DMF, 25°C, $S \cdot m^2/mol$): 4.80. FT-IR (ATR, cm^{-1}): 3093 br *ν*(N−H), 1624 w *ν*(C=N), 1562 m, 1427 m *ν*(C=C, Fc), 1408 m *ν*(C=C), 1057 m *ν*(Ar−Cl), 800 s *ν*(C−H, Fc), 486 s *ν*(Cp−Fe, Fc), 428 m *ν*(Cp−Fe, Fc). UV-Vis (λ_{max} / nm): 446 br, 312 s, 265 m. ^{1}H NMR, δ_H ppm: 12.51 (1H, br, H3), 7.68 (1H, m, H4), 7.12 (1H, m, H6), 6.46 (1H, m, H7), 4.48 (2H, s, H11), 4.22 (2H, s, H12), 4.15 (5H, s, H13). ^{13}C NMR, δ_C ppm: 154.61 (C-2), 139.82 (C-9), 133.49 (C-8), 125.71 (C-5), 121.47 (C-6), 114.98 (C-7), 108.67 (C-4), 73.28 (C-10), 69.98 (C-11), 69.40 (C-12), 67.41 (C-13).

*[Fe(L1)Cl$_3$(H$_2$O)] (**1a**)*

A quantity of 0.337 g **L1** (0.001 mol) was dissolved in methanol (20 mL) in a 50 mL round-bottomed flask and $FeCl_3$ (0.162 g, 0.001 mol) in methanol : water (20 mL : 2 mL) was added to **L1** solution and the mixture was heated gently until 20 mL remained, and then refluxed for 2 hours; the progress of the reaction was monitored with TLC upon completion of the reaction. The product was filtered and kept at room temperature for slow evaporation. The resulting dark green solid was collected by filtration and purified with acetone. A quantity of

0.435 g (78%) of the reaction product **1a** was obtained with m.p. 280–282°C (decomp.). Anal. calcd. for $C_{17}H_{15}Cl_4Fe_2N_2O$ (formula weight: 514.9): C, 39.51; H, 2.93; N, 5.42%; found: C, 40.39; H, 2.78; N, 6.55%. ESI-MS (*m/z*,%): 512.9 ($[(M-2H)]^+$, 18). Magnetic moment, μ_{eff}: 6.20 μ_B. Molar conductivity Λ_M (25°C, $S \cdot m^2/mol$): 30.6. FT-IR (ATR, cm^{-1}): 3304 m, br δ(N−H), 1620 s δ(C=N), 1442 s δ(C=C, Fc), 1409 s δ(C=C), 1062 m δ(Ar−Cl), 810 m δ(C−H, Fc), 478 m δ(Fe−N), 422 m δ(Cp−Fe, Fc). UV-Vis (λ_{max} / nm): 309 s, 293 br, 261 sh, 229 sh.

*[Zn(L1)Cl$_2$(H$_2$O)] (**1b**)*

A quantity of 0.337 g **L1** (0.001 mol) was dissolved in methanol (20 mL) in a 50 mL round-bottomed flask; $ZnCl_2 \cdot 6H_2O$ (0.244 g, 0.001 mol) in methanol : water (40 mL : 4 mL) was added to **L1** solution and the mixture was heated gently until 20 mL remained and then refluxed for 3 hours; the progress of the reaction was monitored with TLC upon completion of the reaction. The mixture was filtered and kept at vacuum for evaporation. The resulting brown solid was collected by filtration and purified with methanol. A quantity of 0.398 g (81%) of the reaction product **1b** was obtained with m.p. 170–172°C (decomp.). Anal. calcd. for $C_{17}H_{15}Cl_3FeN_2OZn$ (formula weight: 490.9): C, 41.59; H, 3.08; N, 5.71%; found: C, 40.82; H, 3.64; N, 5.18%. ESI-MS (*m/z*,%): 535.3 ([M+C_2H_5OH], 100). Magnetic moment, μ_{eff}: 1.10 μ_B. Molar conductivity Λ_M (25°C, $S \cdot m^2/mol$): 20.7. FT-IR (ATR, cm^{-1}): 3203 m, br ν(N–H), 1620*s* ν(C=N), 1427 m ν(C=C, Fc), 1408 m ν(C=C), 1060 w ν(Ar–Cl), 802 w ν(C–H, Fc), 547 w ν(Zn–N), 482 m ν(Cp–Fe, Fc), 426 m ν(Cp–Fe, Fc). UV-Vis (λ_{max} / nm): 450 br, 344 br, 304 sh, 228 sh.

*[Cu(L1)Cl$_2$(H$_2$O)] (**1c**)*

A quantity of 0.337 g of **L1** (0.001 mol) was dissolved in methanol (20 mL) in a 50 mL round-bottomed flask; $CuCl_2 \cdot 2H_2O$ (0.170 g, 0.001 mol) in methanol : water (20 mL : 2 mL) was added to **L1** solution and the mixture was heated gently until 20 mL remained and then refluxed for 3 hours; the progress of the reaction was monitored with TLC upon completion of the reaction. The mixture was filtered and kept in vacuum for evaporation. The resulting brown solid was collected by filtration and purified with methanol/*n*-hexane (30/70) mixture. A quantity of 0.414 g (85%) of the reaction product **1c** was obtained with m.p.> 300°C. Anal. calcd. for $C_{17}H_{15}Cl_3CuFeN_2O$ (formula weight: 486.89): C, 41.75; H, 3.09; N, 5.73%; found: C, 40.98; H, 3.45; N, 5.09%. ESI-MS (*m/z*,%): 487.5 ($[M]^+$, 50.01). Magnetic moment, μ_{eff}: 1.80 μ_B. Molar conductivity Λ_M (25°C, $S \cdot m^2/mol$): 31.0. FT-IR (ATR, cm^{-1}): 3321 m, br ν(N–H), 1581 s ν(C=N), 1444 s ν(C=C, Fc), 1413 s ν(C=C), 1062 m ν(Ar–Cl), 810 m ν(C–H, Fc), 596 m ν(Cu–N), 474 m ν(Cp–Fe, Fc), 430 m ν(Cp–Fe, Fc). UV-Vis (λ_{max} / nm): 290 s, 285 sh, 229 sh.

*[Co(L1)Cl$_2$(H$_2$O)$_3$] (**1d**)*

A quantity of 0.337 g **L1** (0.001 mol) was dissolved in methanol (20 mL) in a 50 mL round-bottomed flask; $CoCl_2 \cdot 6H_2O$ (0.238 g, 0.001 mol) in methanol : water (20 mL : 2 mL) was added to **L1** solution and the mixture was heated gently until 20 mL remained and then refluxed for 2.5 hours; the progress of the reaction was monitored with TLC upon completion of the reaction. The mixture was filtered and kept in vacuum for evaporation. The resulting dark green solid was collected by filtration and purified with ethyl acetate/*n*-hexane (10/90) mixture. A quantity of 0.457 g (88%) of the reaction product **1d** was obtained with m.p.> 300°C. Anal. calcd. for $C_{17}H_{19}Cl_3CoFeN_2O_3$ (formula weight: 518.90): C, 39.23; H, 3.68; N, 5.38%; found: C, 39.47; H, 3.73; N, 4.74%. ESI-MS (*m/z*,%): 520.48 ($[M+1]^+$, 100). Magnetic moment, μ_{eff}: 5.11 μ_B. Molar conductivity Λ_M (25°C, $S \cdot m^2/mol$): 31.8. FT-IR (ATR, cm^{-1}): 3388 m ν(N–H), 1562 m ν(C=N), 1427 m ν(C=C, Fc), 1406 m ν(C=C), 1057 w ν(Ar–Cl), 798 m ν(C–H, Fc), 551 w ν(Co–N), 486 s ν(Cp–Fe, Fc), 426 m ν(Cp–Fe, Fc). UV-Vis (λ_{max} / nm): 436 br, 312 s, 267 sh, 227 sh.

*[Pd(L1)Cl(H$_2$O)]Cl (**1e**)*

A quantity of 0.337 g **L1** (0.001 mol) was dissolved in methanol (20 mL) in a 50 mL round-bottomed flask; $PdCl_2$ (0.177 g, 0.001 mol) and KCl (0.149 g, 0.002 mol) stirred in methanol : water (50 mL : 5 mL) and added to **L1** solution. Reaction mixture was heated gently until 20 mL remained and then refluxed for 4 hours; the progress of the reaction was monitored with TLC upon completion of the reaction. The mixture was filtered and kept in vacuum for evaporation. The resulting brown solid was collected by filtration and purified with *n*-hexane. A quantity of 0.378 g (71%) of the reaction product **1e** was obtained with m.p.> 300°C. Anal. calcd. for $C_{17}H_{15}Cl_3FeN_2OPd$ (formula weight: 531.90): C, 38.38; H, 2.84;N, 5.27%; found: C, 38.97; H, 2.66; N, 5.55%. ESI-MS (*m/z*,%): 551.2 ([M+], 17). Magnetic moment, μ_{eff}: 2.20 μ_B. Molar conductivity Λ_M (25°C, $S \cdot m^2/mol$): 104.1. FT-IR (ATR, cm^{-1}): 3385 m, br ν(N–H), 1620 m ν(C=N), 1438 m ν(C=C, Fc), 1408 m ν(C=C),

1060 w *ν*(Ar–Cl), 802 w *ν*(C–H, Fc), 503 w *ν*(Cp–Fe, Fc), 482 m *ν*(Pd–N), 426 m *ν*(Cp–Fe, Fc). UV-Vis (λ_{max} / nm): 308 s, 265 m, 229 sh.

*(E)-((4-Chloro-2-hydroxyphenylimino)methyl) ferrocene (**HL2**)*

Ferrocenecarboxaldehyde (0.214 g, 0.001 mol) was dissolved in toluene (25 mL) in a 100 mL round-bottomed flask. 2-Amino-4-chlorophenol (0.143 g, 0.001 mol) and CH_3COOH (0.060 g, 0.001 mol, 1.05 g/mL) was stirred in toluene (40 mL); 2-amino-4-chlorophenol mixture was added to ferrocenecarboxaldehyde solution drop-wise during a period of 10 min. The dean stark apparatus was used to increase the reaction yield by removing the water formed from the reaction environment. The reaction mixture was refluxed with dean stark apparatus for 3 hours [10]; the progress of the reaction was monitored with TLC upon completion of the reaction. The reaction was filtered with vacuum. The filtered claret red product was collected by filtration and purified with acetone and then acetonitrile. A quantity of 0.239 g (72%) of the reaction product **HL2** was obtained with m.p. 114–116°C. Anal. calcd. for $C_{17}H_{14}ClFeNO$ (formula weight: 339.6): C, 60.12; H, 4.16; N, 4.12%; found: C, 60.01; H, 4.76; N, 4.98%. ESI-MS (*m/z*,%): 340.0 ($[M]^+$, 100). Molar conductivity Λ_M (25°C, $S \cdot m^2/mol$): 22.9. FT-IR (ATR, cm^{-1}): 3317 br, m *ν*(O–H), 1581 m *ν*(C=N), 1495 m *ν*(C=C, Fc), 1425 m *ν*(C=C), 1090 w *ν*(Ar–Cl), 820 w *ν*(C–H, Fc), 490 w *ν*(Cp–Fe, Fc), 411 m *ν*(Cp–Fe, Fc). UV-Vis (λ_{max} / nm): 442 m, 421 m, 302 sh. ^{1}H NMR, δ_H ppm: 9.88 (1H, s, H1), 8.58 (1H, s, H2), 7.72 (1H, s, H4), 7.16 (1H, s, H6), 6.61 (1H, m, H7), 4.80 (2H, m, H11), 4.66 (2H, m, H12), 4.29 (5H, s, H13). ^{13}C NMR, δ_H ppm: 163.17 (C-2), 148.88 (C-8), 142.81 (C-9), 126.42 (C-4), 122.59 (C-5), 115.73 (C-6), 113.65 (C-7), 79.22 (C-10), 72.82 (C-11), 71.25 (C-12), 69.34 (C-13).

*$[Fe(HL2)Cl_3(H_2O)]\cdot H_2O$ (**2a**)*

A quantity of 0.339 g (0.001 mol) **HL2** was dissolved in methanol (20 mL) in a 50 mL round-bottomed flask; $FeCl_3$ (0.162 g, 0.001 mol) in methanol : water (20 mL : 2 mL) was added to **HL2** solution and the mixture was heated gently until 20 mL remained and then refluxed for 4 hours; the progress of the reaction was monitored with TLC upon completion of the reaction. The brown precipitate was filtered and kept at room temperature for slow evaporation. The obtained brown precipitate was washed a few times with methanol, and dried under vacuum. A quantity of 0.403 g (75%) of the reaction product **2a** was obtained with m.p.> 300°C. Anal. calcd. for $C_{17}H_{18}Cl_4Fe_2NO_3$ (formula weight: 537.8): C, 37.96; H, 3.37; N, 2.60%; found: C, 37.23; H, 3.98; N, 2.54%. ESI-MS (*m/z*,%): 538.8 ($[M+H]^+$, 46), ($[M-H_2O]$, 15). Magnetic moment, μ_{eff}: 5.70 μ_B. Molar conductivity Λ_M (25°C, $S \cdot m^2/mol$): 37.9. FT-IR (ATR, cm^{-1}): 3211 s, br *ν*(O–H), 1614 m *ν*(C=N), 1492 m *ν*(C=C, Fc), 1417 m *ν*(C=C), 1118 w *ν*(Ar–Cl), 801 m *ν*(C–H, Fc), 747 m *ν*(Fe–O), 476 w *ν*(Cp–Fe, Fc), 467 w *ν*(Fe–N), 428 w *ν*(Cp–Fe, Fc). UV-Vis (λ_{max} / nm): 340 *br*, 260 *s*, 234 *sh*.

*$[Zn(HL2)Cl_2]\cdot H_2O$ (**2b**)*

A quantity of 339 g (0.001 mol) **HL2** was dissolved in methanol (20 mL) in a 50 mL round-bottomed flask; $ZnCl_2 \cdot 6H_2O$ (0.244 g, 0.001 mol) in methanol : water (40 mL : 4 mL) was added to **HL2** solution and the mixture was heated gently until 20 mL remained and then refluxed for 2 hours; the progress of the reaction was monitored with TLC upon completion of the reaction. The reaction mixture was filtered and allowed to cool. The resulting claret red precipitate was washed with a few times with *n*-hexane and dried under vacuum. A quantity of 0.445 g (90%) of the reaction product **2b** was obtained with m.p. 120–122°C. Anal. calcd. for $C_{17}H_{16}Cl_3FeNO_2Zn$ (formula weight: 490.9): C, 41.34; H, 3.27; N, 2.84%; found: C, 41.78; H, 3.07; N, 2.76%. ESI-MS (*m/z*,%): 490.4 ($[M]^+$, 48). Magnetic moment, μ_{eff}: 1.90 μ_B. Molar conductivity Λ_M (25°C, $S \cdot m^2/mol$): 14.1. FT-IR (ATR, cm^{-1}): 3369 s, br *ν*(O–H), 1597 s *ν*(C=N), 1479 m *ν*(C=C, Fc), 1456 m *ν*(C=C), 1107 w *ν*(Ar–Cl), 812 m *ν*(C–H, Fc), 570 w *ν*(Zn–N), 471 s *ν*(Zn–O), 403 w *ν*(Cp–Fe, Fc). UV-Vis (λ_{max} / nm): 437 *br*, 418 *br*, 301 *sh*, 234 *s*.

*$[Cu(HL2)Cl_2]\cdot H_2O$ (**2c**)*

A quantity of 0.339 g (0.001 mol) **HL2** was dissolved in methanol (20 mL) in a 50 mL round-bottomed flask; $CuCl_2 \cdot 2H_2O$ (0.170 g, 0.001 mol) in methanol : water (30 mL : 3 mL) was added to **HL2** solution and the mixture was heated gently until 20 mL remained and then refluxed for 2 hours; the progress of the reaction was monitored with TLC upon completion of the reaction. The reaction mixture was filtered and allowed to cool. The resulting brown precipitate was collected by filtration and purified with dichloromethane/*n*-hexane (20/80) mixture. A quantity of 0.340 g (69%) of the reaction product **2c** was obtained with m.p. 240–242°C. Anal. calcd. for $C_{17}H_{16}Cl_3CuFeNO_2$ (formula weight: 492.1): C, 41.49; H, 3.28; N, 2.85%; found: C, 40.93; H, 3.78; N, 2.14%. ESI-MS (*m/z*,%): 491.0 ($[M-1]^+$, 54.5). Magnetic moment, μ_{eff}: 1.72 μ_B. Molar conductivity Λ_M (25°C,

S·m^2/mol): 26.3. FT-IR (ATR, cm^{-1}): 3319 m, br *ν*(O–H), 1568 m *ν*(C=N), 1492 m *ν*(C=C, Fc), 1423 m *ν*(C=C), 1091 w *ν*(Ar–Cl), 819 w *ν*(C–H, Fc), 667 w *ν*(Cu–N), 442 w *ν*(Cu–O), 422 w *ν*(Cp–Fe, Fc), 408 w *ν*(Cp–Fe, Fc). UV-Vis (λ_{max} / nm): 420 br, 290 br, 229 sh.

[Co(HL2)Cl$_2$(H$_2$O)$_2$]·H$_2$O ***(2d)***

A quantity of 0.339 g (0.001 mol) **HL2** was dissolved in methanol (20 mL) in a 50 mL round-bottomed flask; $CoCl_2 \cdot 6H_2O$ (0.238 g, 0.001 mol) in methanol : water (60 mL : 6 mL) was added to **HL2** solution and the mixture was heated gently until 20 mL remained and then refluxed for 4 hours; the progress of the reaction was monitored with TLC upon completion of the reaction. The reaction mixture was filtered and kept in vacuum for evaporation. The resulting brown solid was collected by filtration and purified with methanol/*n*-hexane (40/60) mixture. A quantity of 0.438 g (84%) of the reaction product **2d** was obtained with m.p. 148–150°C (decomp.). Anal. calcd. for $C_{17}H_{20}Cl_3CoFeNO_4$ (formula weight: 521.90): C, 39.00; H, 3.85; N, 2.68%; Found: C, 38.42; H, 4.03; N, 1.98%. ESI-MS (*m/z*,%): 520.2 ([M-1]$^+$, 100). Magnetic moment, μ_{eff}: 4.41 BM. Molar conductivity Λ_M (25°C, S·m^2/mol): 44.6. FT-IR (ATR, cm^{-1}): 3097 m *ν*(O–H), 1570 m *ν*(C=N), 1485 m *ν*(C=C, Fc), 1410 m *ν*(C=C), 1105 w *ν*(Ar–Cl), 818 m *ν*(C–H, Fc), 586 w *ν*(Co–N), 515 w *ν*(Co–O), 478 m *ν*(Cp–Fe, Fc), 457 m *ν*(Cp–Fe, Fc). UV-Vis (λ_{max} / nm): 442 br, 421 br, 259 s.

[Pd(HL2)Cl(H$_2$O)]Cl ***(2e)***

A quantity of 0.339 g (0.001 mol) **HL2** was dissolved in methanol (20 mL) in a 50 mL round-bottomed flask. $PdCl_2$ (0.177 g, 0.001 mol) and KCl (0.149 g, 0.002 mol) stirred in methanol : water (50 mL : 5 mL) and added to **HL2** solution. The reaction mixture was heated gently until 20 mL remained and then refluxed for 5 hours; the progress of the reaction was monitored with TLC upon completion of the reaction. The reaction mixture was filtered and allowed to cool. The resulting brown precipitate was collected by filtration and purified with dichloromethane/n-hexane (30/70) mixture. A quantity of 0.378 g (70%) of the reaction product **2e** was obtained with m.p.> 300°C. Anal. calcd. for $C_{17}H_{16}Cl_3FeNO_2Pd$ (formula weight: 532.90): C, 38.17; H, 3.01; N, 2.62%; found: C, 38.87; H, 3.57; N, 2.32%. ESI-MS (*m/z*,%): 532.0 ([(M-H)]$^+$, 100). Magnetic moment, μ_{eff}: 0.00 μ_B. Molar conductivity Λ_M (25°C, S·m^2/mol): 73.1. FT-IR (ATR, cm^{-1}): 3389 m, br *ν*(O–H), 1601 m *ν*(C=N), 1479 w *ν*(C=C, Fc), 1410 w *ν*(C=C), 1107 w *ν*(Ar–Cl), 814 m *ν*(C–H, Fc), 471 m *ν*(Pd–N), 430 w *ν*(Cp–Fe, Fc), 409 w *ν*(Pd–O). UV-Vis (λ_{max}/nm): 425 m,br, 229 s.

Antibacterial activity evaluation

The synthesized ligands and their complexes were tested against one Gram-positive and one Gram-negative bacteria. The reference strains *Staphylococcus aureus* ATCC 25923 and *Escherichia coli* ATCC 25922 were obtained from the Turkish Republic General Directorate of Public Health, Ankara, Turkey. The bacteria were first grown on blood agar containing 5% sheep blood at 37°C. Later, the bacterial cell concentrations were adjusted to 0.5 McFarland and the bacteria were inoculated on Mueller Hinton agar plates under aseptic conditions using sterile cotton swabs. According to Balouiri, M. *et al*. the agar well diffusion method was then applied by forming 6 mm wells with the help of sterile pipette tips [11]. Different concentrations of the ligand and complexes were prepared by two-fold serial dilutions in DMSO starting from 256 mg/mL to 1 mg/mL. DMSO was also used as the negative control while 10 µg Gentamicin sulphate (Sigma-Aldrich, Darmstadt, Germany) was used as positive control. A volume of 50 µL of each concentration was added to the wells. The plates were kept at 37±0.1°C for 24 hours. After a careful visual inspection, the zones of antibacterial activity were determined and the diameter of clear zone around each well was measured in mm as an indicator of antibacterial activity of each compound and were compared with that of the standard antibiotic Gentamicin.

Results and discussion

Synthesis and characterisation

Synthesis of the **L1** and **HL2** ligands were given in Schemes 1 and 2, ferrocenecarboxaldehyde and 4-chloro-*o*-phenylenediamine (for **L1**) or 2-amino-4-chlorophenol (for **HL2**) were reacted in a 1:1 mole ratio. Also, the ligands and metal chlorides ($FeCl_3$, $CoCl_2 \cdot 6H_2O$, $CuCl_2 \cdot 2H_2O$, $ZnCl_2 \cdot 6H_2O$ and $PdCl_2$) reacted at a mole ratio of 1:1 to produce dinuclear metal complexes. **L1** is a monodentate ligand, and coordinates with metal ions through the imine nitrogen atom (C=N) [2]. Schiff base ligand (**HL2**) has a bidentate coordination. It can binary "grab" a metal atom over oxygen and nitrogen atoms [7]. The structure of ligands and complexes were characterized by the melting point, elemental analysis, FT-IR, ^{1}H and ^{13}C NMR, UV-Vis

spectroscopy and mass spectrometry (ESI-MS) techniques. Molar conductivity and magnetic moment measurements were applied for further characterization of the complexes. A generalisation of analytical data and physical properties of ligands and complexes is given in Table S1 (see the Supplementary material).

Infrared spectroscopy characterization

Investigation of FT-IR peaks is important for comparison of ligand and metal complexes. Especially, C=N bands are characteristic for benzimidazoles, and the C=N and O–H bands for Schiff bases. The interaction between ligand and metal occur with these functional groups.

In the FT-IR spectra of the ligands, the medium bands at 1624 cm^{-1} (**L1**) and 1584 cm^{-1} (**HL2**) must belong to the C=N groups. The corresponding wavenumbers in the complexes are detected at the 1620–1562 cm^{-1} (**1a-e**) and 1614–1568 cm^{-1} ranges (**2a-e**). The C=N stretching frequencies of the complexes has been changed as it binds with metals *via* the C=N nitrogen atom [12,13].

For the functional ferrocene group, the characteristic C–H (out-of-plane) peaks were observed at 700–830 cm^{-1} range, C=C stretching at 1420–1470 cm^{-1} range, Cp–Fe stretching at around 400 and 500 cm^{-1} [14]. The NH band, which can be observed at 3093 cm^{-1} in the benzimidazole ligand, shifts to 3300 cm^{-1} upon complex formation [15]. The O–H peak for **HL2** is observed at 3317 cm^{-1} [16]. The broad band between 3000-2500 cm^{-1} in the complexes could be attributed to the hydrogen bonding because of the coordinated and uncoordinated (lattice) water molecules. However, in the literature, it is seen that the O–H peak in the complexes of some Schiff bases with metals originates from the water in the environment [16,17]. Therefore, the O–H peaks in the compounds (**2a-e**) between 3389 and 3098 cm^{-1} could belong to H_2O. The appearance of the characteristic metal-nitrogen and metal-oxygen vibrations indicates the bidentate bonding of the Schiff base ligand to the metal ion [3,16-21].

NMR spectroscopy characterization

NMR spectra of the Pd(II) and Zn(II) complexes could not be recorded because of the paramagnetic effect of the ferrocene group. The characteristic single N–H signal of **L1** was observed at 12.51 ppm [22]. Phenolic OH and azomethine CH=N protons of Schiff base ligand (**HL2**) give singlet at 9.88 and 8.58 ppm, respectively [12,21]. The protons of the benzene ring of benzimidazole and Schiff base ligands were found in the range 6.46 to 7.72 ppm [23].

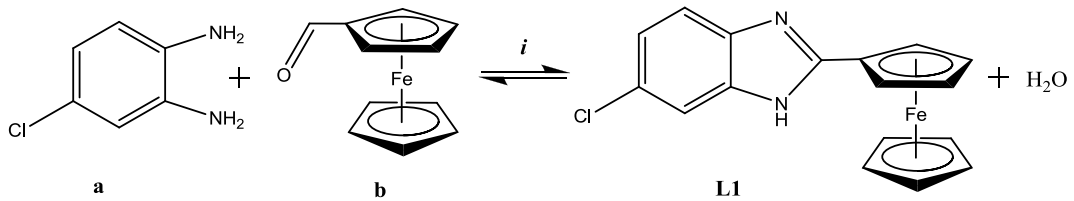

Reagent and conditions: i) EtOH solvent, H_3BO_3 catalyst, reflux 2 hours, 71%.
(a) 4-chloro-*o*-phenylenediamine; *(b)* ferrocenecarboxaldehyde

Scheme 1. Synthesis of 6-chloro-2-ferrocenyl-1*H*-benzimidazole (L1) ligand.

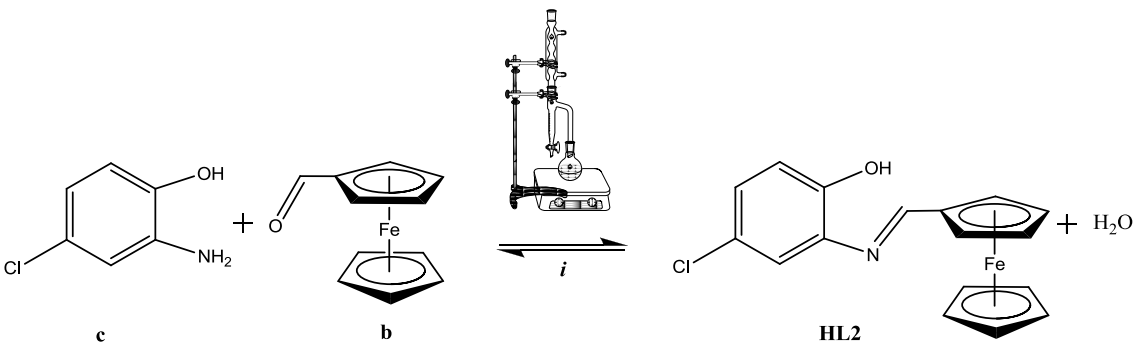

Reagent and conditions: i) toluene / acetic acid solvent mixture, reflux with Dean Stark apparatus 3 hours, 72%.
(c) 2-amino-4-chlorophenol; *(b)* ferrocenecarboxaldehyde

Scheme 2. Synthesis of (*E*)-((4-chloro-2-hydroxyphenylimino)methyl)ferrocene (HL2) ligand.

The chemical structure of the ligands, **L1** and **HL2,** are shown in Figure 1. There are 3 different types of protons in the ferrocene moiety H11 (two protons), H12 (two protons) and H13 (five protons). Chemical shift values of these protons are compatible with the literature [24].

The chemical shift values of the benzene rings of **L1** and **HL2** are at the range of 108.67-126.42 ppm for C4, C6 and C7 carbon atoms, and 125.71-122.59 ppm for substituted C5 carbons. Chemical shift values for the quaternary carbon atoms, C8 and C9, on the benzene ring, were observed at 133.49 ppm and 139.82 ppm (**L1**), and at 142.81 and 148.88 ppm (**HL2**), respectively. The chemical shift value for the benzimidazole ligand (**L1**) of the C2 (C=N) carbon was found to be 154.61 ppm and 163.17 ppm for the Schiff base (**HL2**) [22,25-27]. There are four different types of carbons in the ferrocene moiety of **L1** and **HL2**: C10 (one carbon), C11 (two carbons), C12 (two carbons) and C13 (five carbons). The ipso-carbon (C10) on the substituted Cp ring is observed at 73.29 ppm and 79.22 ppm for **L1** and **HL2**, respectively. C11 relates to two carbons adjacent to the carbon (C10) on the cyclopentadienyl (C_5H_4) ring with ferrocene bonds. C12, other protons in the cyclopentadienyl ring where ferrocene is attached to benzimidazole. The third type are the C13 carbons in the unsubstituted cyclopentadienyl (C_5H_5) ring. Chemical shift values of these carbons are compatible with the literature (Figures S1-S4) [25-27].

UV-Vis spectra analysis

The peaks observed in the low range (200–300 nm) represent the transition $\pi \rightarrow \pi^*$ in the aromatic rings of the ligands and complexes [25-27]. The 300–350 nm bands involve $\pi \rightarrow \pi^*$ transitions of the C=N group in Schiff base compounds containing ferrocene. In addition to this band, a weaker absorption is observed in the 430-460 nm range. This band indicates *d–d* transitions in ferrocene-containing complexes but it is not always observed. The weak *d–d* transitions found in Schiff bases cannot be clearly determined in UV-Vis spectroscopy (Figures 2 and 3) [13,28].

Metal ligand interaction in Fe(III) complexes can be observed as a shoulder band at 300 nm (**1a**) and 340 nm (**2a**) in the UV-vis spectrum [29]. Since Zn(II) complexes (**1b**, **2b**) have d^{10} electronic configuration, the *d–d* transition was not observed. The band observed around 300-350 nm is due to the charge transfer transition between the ligand and the Zn(II) ion (L→M; O→M) [30].

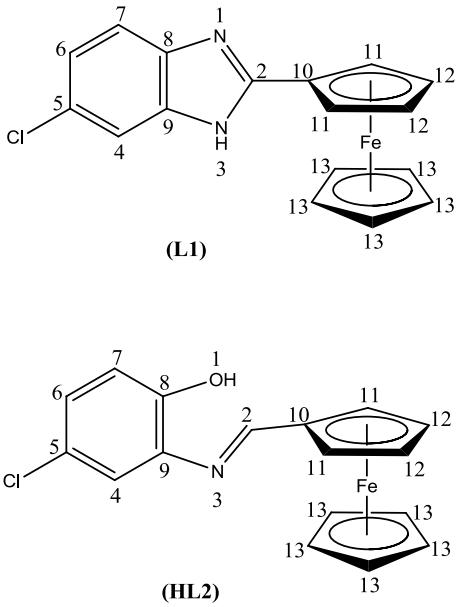

Figure 1. The chemical structure of the L1 and HL2 ligands.

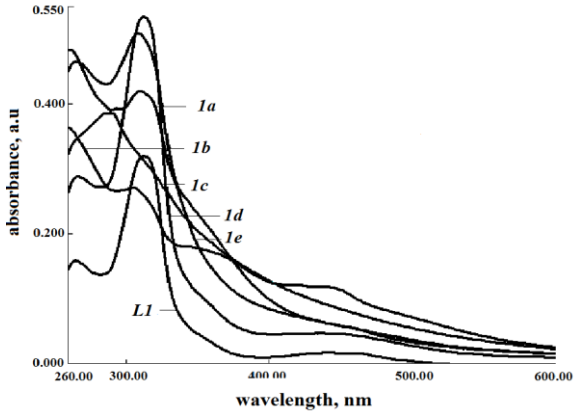

Figure 2. UV-Vis spectra of L1, 1a, 1b, 1c, 1d and 1e at a concentration of 10^{-2} M in DMSO.

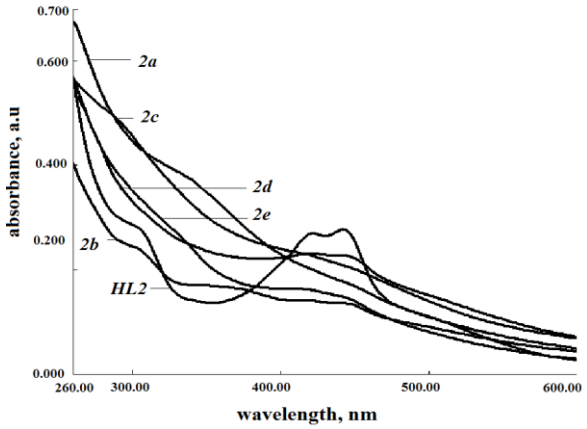

Figure 3. UV-Vis spectra of HL2, 2a, 2b, 2c, 2d and 2e at a concentration of 10^{-2} M in DMSO.

The observed band at 290 nm (**1c**) and shoulder at 300 nm (**2c**) in the spectra of Cu(II) complexes is attributed to the charge transfer between metal and ligands assuming a square-planar configuration [31]. Co(II) (**1d**, **2d**) complexes have six coordinates and have octahedral structures, if **1d** and **2d** complexes have a $2a \rightarrow 1g$ transition, they will present a weak band at 530 nm. Absorptions between 250 and 330 nm are due to the ligand to metal charge transfer transition [32]. Pd(II) complexes (**1e**, **2e**) bonding with the ligand give a band at 280–340 nm in the UV-Vis spectrum. Non-bonding Pd(II) halides give bands at 450 nm [33].

Molar conductivity and magnetic moment measurements

Molar conductivity data of the complexes give useful information about the structure of the complexes. According to the molar conductivity data, Pd(II) complexes having molar conductivity values of 104.1 and 73.1 $S \cdot m^2$/mol, respectively for **1e** and **2e**, are 1:1 electrolytes. Only these two complexes react with $AgNO_3$ to form the AgCl salt. There was no precipitation of AgCl in the other complexes, indicating that the chloride anions are inside the coordination sphere of the complexes. Fe(III), Cu(II), Zn(II) and Co(II) complexes are not electrolytes since their molar conductivity value is in the range of 20.7-44.6 $S \cdot m^2$/mol. The molar conductivity values for the 1:1 electrolyte in DMF should generally be higher than 50 $S \cdot m^2$/mol [33,34].

Room temperature magnetic moment values of complex compounds match the predicted geometry and structural properties. Magnetic moment values (μ_{eff}) of the complexes are shown in the Experimental section. Many paramagnetic compounds containing ferrocene functional groups exhibit higher magnetic moment values than expected [35]. Also, diamagnetic Pd^{2+} complexes may show paramagnetic character since they have ferrocene. This unexpected situation indicates that the diamagnetic character of Fe^{2+} in the ferrocene group disappears with the unpaired electron pair found in ferrocene [34-36].

The magnetic moment values of Fe^{3+} complexes are 5.6-6.1 μ_B for high spin and 1.8-2.1 μ_B for low spin octahedral geometry [34-36]. The magnetic moment values of **1a** and **2a** are 6.2 and 5.7 μ_B respectively so their structures are estimated to be octahedral with high spin. Due to the diamagnetism of Zn^{2+} and Pd^{2+} ions, the μ_B values of the complexes **1b**, **2b**, **1e** and **2e** must be zero. However, the μ_B values both of the complexes are positive due to paramagnetic effect of the ferrocene group [34-36]. Magnetic moment values of Cu^{2+} complexes, **1c** and **2c**, are 1.8 μ_B and 1.72 μ_B respectively, corresponding to one unpaired electron expected for d^9 square-planar Cu^{2+} complexes [7,18-20]. Magnetic moment values of the Co^{2+} complexes are found as 5.11 μ_B for **1d** and 4.41 μ_B for **2d**. Co^{2+} complexes in the range of 4.3-5.2 μ_B in octahedral compounds are obtained [34-36]. The d^8 electron configuration complexes are generally square planar, and in a small number of samples are tetrahedral. Although the coordination number is 3 in the empirical formulas of **1e** and **2e** in the results of the elemental analysis, these complexes may be in dimeric structure. In this case, the coordinated Cl anion can act as a bridging ligand and become a 4-coordinated structure. Therefore, it is highly probable that the Pd^{2+} complexes, **1e** and **2e**, are square planar.

Antibacterial activity evaluation of the complexes

The antibacterial activity of the ligands and the complexes was evaluated against a Gram-positive (*Staphylococcus aureus*) and a Gram-negative (*Escherichia coli*) bacterial strains. These bacteria are members of the normal flora of humans. Some strains of these bacteria have become resistant to many antibiotics. This situation is especially important for the normal flora bacteria which have developed to be antibiotic resistant and result in nosocomial infections [37,39]. Benzimidazoles have a potential to be used as antibacterial agents as alternative to current antibiotics to which bacteria gain resistance day by day [40]. Results of the antibacterial evaluation of the obtained compounds are summarized in Table 2.

Table 2

Concentration (mg/mL) of the compound showing significant inhibition compared to Gentamicin.

Compounds	*E. coli*	*S. aureus*
L1	>256	>256
1a	>256	>256
1b	128	16
1c	64	64
1d	64	2
1e	32	8
HL2	64	16
2a	128	64
2b	128	4
2c	32	64
2d	32	32
2e	64	128

The minimum inhibitory concentration of Gentamicin antibiotic for the bacteria used in this study was given to be less than 2 mg/mL by The European Committee on Antibacterial Susceptibility Testing (EUCAST) [41]. If the zone diameter of the compound was 30-50% of the Gentamicin inhibition zone, which was 16 mm for *E. coli* and 20 mm for *S. aureus*, the inhibition was accepted as significant. The concentration which exerts a significant inhibition compared to the reference antibiotic is given in Table 2.

The negative control DMSO was ineffective in inhibiting all the bacterial strains, as expected [42,43]. **L1** was ineffective against both bacteria even at the highest concentration tested in this study (>256 mg/mL). The complexes of **L1** showed considerably high antibacterial activity, except for **1a**. This result can be explained by Tweedy's Chelation Theory, which states that the activities of chemical compounds increase when they form complexes [42,43].

Chelation decreases the polarity of the metal as a partial positive charge of the metal atom is shared with the donor groups and possible electron delocalization occurs over the entire ring. This increases the lipophilic character of the chelates, which promotes their passage through the lipid layers of the bacterial membrane. The complexes of both ligands have a higher inhibition effect on *Staphylococcus aureus*. Moreover, the bacteriostatic effects of the complexes **1d**, **1e**, **2b**, **2d** and **2e** on *Staphylococcus aureus* are noticeable. The full potentials of the complexes could not be totally observable due to the precipitation of the complexes dissolved in DMSO when came across with the water molecules present in agar. The precipitations of the complexes are especially obvious starting from the concentration of 16 mg/mL. Nevertheless, the order of activities can be shown as **1d** > **1e** > **1b** > **1c** > **1a** = **L1** for *Staphylococcus aureus* and **1e** > **1d** > **1c** > **1b** > **1a** = **L1** for *Escherichia coli*. The order for **HL2** and its complexes is as follows: **2b** > **HL2** > **2d** > **2a** = **2c** > **2e** for *Staphylococcus aureus* and **2c** = **2d** > **2e** > **HL2** > **2a** = **2b** for *Escherichia coli*. The effect of a structural change between **L1** and **HL2** was very obvious, the **L1** was ineffective against bacteria, however, **HL2** was effective on both bacteria, especially on *Staphylococcus aureus*. This can be explained by the cell wall differences between Gram-positive and Gram-negative bacteria (Figures S5-S8, Supplementary material). The cell wall of Gram-positive bacteria is more permeable and therefore some antibacterial agents can act more effectively on Gram-positive bacteria [42]. The high activity of **1d** (Co^{2+} complex) and **2b** (Zn^{2+} complex) against *Staphylococcus aureus* (2 and 4 mg/mL, respectively), is quite remarkable.

Conclusions

In this study, a ferrrocenyl benzimidazole derivative, 6-chloro-2-ferrocenyl-1*H*-benzimidazole (**L1**) and a ferrocenyl Schiff base, (*E*)-((4-chloro-2-hydroxyphenylimino)methyl) ferrocene (**HL2**) ligands and their complexes with Fe(III), Co(II), Cu(II), Zn(II) and Pd(II) chloride were synthesized and characterized. All complexes reacted in a 1:1 metal:ligand ratio.

Molar conductivity data showed that Fe(III), Cu(II), Zn(II) and Co(II) complexes are not electrolytes whereas the Pd(II) complexes are 1:1 electrolyte. According to the obtained data, it is estimated that Fe(III) and Co(II) complexes have octahedral geometry, Zn(II) and Cu(II) complexes manifest tetrahedral geometry and Pd(II) complexes present square plane geometry. Due to the characteristics of the ligands, **HL2** complexes have a chelate structure whereas the complexes of **L1** are not. Antibacterial activity of the ligands and the complexes were tested towards *Escherichia coli* and *Staphylococcus aureus*. It was observed that especially benzimidazole derivative complexes (**1b** – **1e**) show higher activity compared to the ligand and this situation is considered to be related to the non-chelate structures of benzimidazole compound complexes. The activities of **1d** (Co^{2+} complex) and **2b** (Zn^{2+} complex) against *Staphylococcus aureus* (2 and 4 µg/mL, respectively), are notable for being considerably higher than the others.

Acknowledgments

This work was supported by Scientific Research Projects Coordination Unit of Istanbul University – Cerrahpasa, project no.: FDK-2017-23684.

Supplementary information

Supplementary data are available free of charge at http://cjm.asm.md as PDF file.

References

1. Patra, M.; Gasser, G. The medicinal chemistry of ferrocene and its derivatives. Nature Reviews Chemistry, 2017, 1, 0066, pp. 1–12. DOI: https://doi.org/10.1038/s41570-017-0066
2. Cunningham, L.; Benson, A.; Guiry, P.J. Recent developments in the synthesis and applications of chiral ferrocene ligands and organocatalysts in

asymmetric catalysis. Organic & Biomolecular Chemistry, 2020, 18(46), pp. 9329–9370. DOI: https://doi.org/10.1039/D0OB01933J
3. Astruc, D. Why is ferrocene so exceptional? European Journal of Inorganic Chemistry, 2017, 1, pp. 6–29. DOI: https://doi.org/10.1002/ejic.201600983
4. Wagner, E.C.; Millet, W.H. Benzimidazole. Organic Syntheses, 1939, 19, pp. 12–15. DOI: https://doi.org/10.15227/orgsyn.019.0012
5. Zapata, F.; Caballero, A.; Espinosa, A.; Tarraga, A.; Molina, P. Triple channel sensing of Pb(II) ions by a simple multiresponsive ferrocene receptor having a 1-deazapurine backbone. Organic Letters, 2008, 10(1), pp. 41–44. DOI: https://doi.org/10.1021/ol702541y
6. Vigato, P.A.; Tamburini, S. The challenge of cyclic and acyclic Schiff bases and related derivatives. Coordination Chemistry Reviews, 2004, 248(17–20), pp. 1717–2128. DOI: https://doi.org/10.1016/j.cct.2003.09.003
7. Kumar, S.; Dhar, D.N.; Saxena, P.N. Applications of metal complexes of Schiff bases - a review. Journal of Scientific & Industrial Research, 2009, 68, pp. 181–187. http://nopr.niscpr.res.in/bitstream/123456789/3170/1/JSIR%2068%283%29%20181-187.pdf
8. Karimi-Jaberi, Z.; Amiri, M. An efficient and inexpensive synthesis of 2-substituted benzimidazoles in water using boric acid at room temperature. E-Journal of Chemistry, 2012, 9(1), pp. 167–171. DOI: https://doi.org/10.1155/2012/793978
9. Vazzana, I.; Terranova, E.; Mattioli, F.; Sparatore, F. Aromatic Schiff bases and 2,3-disubstituted-1,3-thiazolidin-4-one derivatives as antiinflammatory agents. Arkivoc, 2004, 5, pp. 364–374. DOI: https://doi.org/10.3998/ark.5550190.0005.531
10. Balouiri, M.; Sadiki, M.; Ibnsouda, S.K. Methods for *in vitro* evaluating antimicrobial activity: a review. Journal of Pharmaceutical Analysis, 2016, 6(2), pp. 71–79. DOI: https://doi.org/10.1016/j.jpha.2015.11.005
11. Tavman, A. Synthesis, spectral characterization of 2-(5-methyl-1*H*-benzimidazol-2-yl)-4-bromo/nitro-phenols and their complexes with zinc(II) ion, and solvent effect on complexation. Spectrochimica Acta Part A, 2006, 63(2), pp. 343–348. DOI: https://doi.org/10.1016/j.saa.2005.05.020
12. Tavman, A.; Agh-Atabay, N.M.; Neshat, A.; Gucin, F.; Dulger, B.; Haciu, D. Structural characterization and antimicrobial activity of 2-(5-*H*/methyl-1*H*-benzimidazol-2-yl)-4-bromo/nitro-phenol ligands and their $Fe(NO_3)_3$ complexes. Transition Metal Chemistry, 2006, 31, pp. 194–200. DOI: https://doi.org/10.1007/s11243-005-6368-1
13. Garnovskii, A.D.; Sennikova, E.V.; Kharisov, B.I. Coordination aspects in modern inorganic chemistry. The Open Inorganic Chemistry Journal, 2009, 3(1), pp. 1–20. DOI: https://doi.org/10.2174/1874098700903010001
14. Hariprasath, K.; Deepthi, B.; Sudheer Babu, I.; Venkatesh, P.; Sharfudeen, S.; Soumya, V. Metal complexes in drug research - a review. Journal of Chemical and Pharmaceutical Research, 2010, 2(4), pp. 496–499. https://www.jocpr.com/articles/metal-complexes-in-drug-research--a-review.pdf
15. Elseman, A.M.; Shalan, A.E.; Rashad, M.M.; Hassan, A.M.; Ibrahim, N.M.; Nassar, A.M. Easily attainable new approach to mass yield ferrocenyl Schiff base and different metal complexes of ferrocenyl Schiff base through convenient ultrasonication-solvothermal method. Journal of Physical Organic Chemistry, 2017, 30(6), pp. e3639–e3648. DOI: https://doi.org/10.1002/poc.3639
16. Socrates, G. Infrared and Raman Characteristic Group Frequencies. John Wiley & Sons Ltd.: New York, USA, 2001, 366 p. ISBN: 0-471-85298-8
17. Saxena, A.K.; Saxena, S.; Rai, A.K. Some titanium(IV) complexes of 1,3-dihydro-1,3-dioxo-∝-(Substituted)-2*H*-isoindole-2-acetates. Synthesis and Reactivity in Inorganic Metal-Organic Chemistry, 1990, 20(1), pp. 21–37. DOI: https://doi.org/10.1080/00945719008049867
18. Amjad, M.; Sumrra, S.H.; Akram, M.S.; Chohan, Z.H. Metal-based ethanolamine-derived compounds: a note on their synthesis, characterization and bioactivity. Journal of Enzyme Inhibition and Medicinal Chemistry, 2016, 31(S4), pp. 88–97. DOI: https://doi.org/10.1080/14756366.2016.1220375
19. Tendero, M.J.L.; Benito, A.; Lloris, J.M.; Martinez-Máñez, R.; Soto, J.; Paya, J.; Edwards, A.J.; Raithby, P.R. Synthesis and characterisation of the new diaza ferrocene macrocycle 1,1′-(2,6-diazahepta-1,6-diene) ferrocene and its parent amine 1,1′-(2,6-diazaheptane) ferrocene. Inorganica Chimica Acta, 1996, 247(1), pp. 139–142. DOI: https://doi.org/10.1016/0020-1693(95)04952-5
20. Cinarli, A.; Gürbüz, D.; Tavman, A.; Birteksöz, A.S. Synthesis, spectral characterizations and antimicrobial activity of some Schiff bases of 4-chloro-2-aminophenol. Bulletin of the Chemical Society of Ethiopia, 2011, 25(3), pp. 407–417. DOI: https://doi.org/10.4314/bcse.v25i3.68593
21. Yamamoto, T.; Sugiyama, K.; Kanbara, T.; Hayashi, H.; Etori, H. Preparation and properties of π-conjugated poly(benzimidazole-4,7-diyl)s. Macromolecular Chemistry and Physics, 1998, 199(9), pp. 1807–1813. DOI: https://doi.org/10.1002/(SICI)1521-3935(19980901)199:9<1807::AID-MACP1807>3.0.CO;2-2
22. D'Antona, N.; Morrone, R.; Gambera, G.; Pedotti, S. Enantiorecognition of planar "metallocenic" chirality by a nitrile hydratase/amidase bienzymatic system. Organic & Biomolecular Chemistry, 2016, 14, pp. 4393–4399. DOI: https://doi.org/10.1039/C6OB00689B

23. Toro, P.; Klahn, A.H.; Pradines, B.; Lahoz, F.; Pascual, A.; Biot, C.; Arancibia, R. Organometallic benzimidazoles: Synthesis, characterization and antimalarial activity. Inorganic Chemistry Communications, 2013, 35, pp. 126–129. DOI: https://doi.org/10.1016/j.inoche.2013.06.019
24. Liu, Y.-T.; Lian, G.-D.; Yin, D.-W.; Su, B.-J. Synthesis, characterization and biological activity of ferrocene-based Schiff base ligands and their metal (II) complexes. Spectrochimica Acta Part A, 2013, 100, pp. 131–137. DOI: https://doi.org/10.1016/j.saa.2012.03.049
25. Shabbir, M.; Akhter, Z.; Ahmad, I.; Ahmed, S.; Bolte, M.; Ismail, H.; Mirza, B. Ferrocene-based Schiff bases copper(II) complexes: synthesis, characterization, biological and electrochemical analysis. Inorganica Chimica Acta, 2017, 463, pp. 102–111. DOI: https://doi.org/10.1016/j.ica.2017.04.034
26. Tavman, A.; Cinarli, A.; Gürbüz, D.; Birteksöz, A.S. Synthesis, characterization and antimicrobial activity of 2-(5-H/Me/F/Cl/NO_2-1*H*-benzimidazol-2-yl)-benzene-1,4-diols and some transition metal complexes. Journal of the Iranian Chemical Society, 2012, 9(5), pp. 815–825. DOI: https://doi.org/10.1007/s13738-012-0098-z
27. Shi, Y.-C.; Yang, H.-M.; Shen, W.-B.; Yan, C.-G.; Hu, X.-Y. Syntheses and crystal structures of ferrocene-containing enaminones and their copper complexes. Polyhedron, 2004, 23(1), pp. 15–21. DOI: https://doi.org/10.1016/j.poly.2003.08.017
28. Berreau, L.M. Coordination and bioinorganic chemistry of aryl-appended *tris*(2-pyridylmethyl) amine liands. Comments on Inorganic Chemistry, 2007, 28(3-4), pp. 123–171. DOI: https://doi.org/10.1080/02603590701572940
29. Abd-Elzaher, M.M. Synthesis, characterization, and antimicrobial activity of cobalt(II), nickel(II), copper(II) and zinc(II) complexes with ferrocenyl Schiff bases containing a phenol moiety. Applied Organometallic Chemistry, 2004, 18(4), pp. 149–155. DOI: https://doi.org/10.1002/aoc.608
30. El-Tabl, A.S.; Issa, R.M. Preparation and characterization of new nickel(II), cobalt(II) and copper(II) complexes of 3,11-diacetyl-2,12-dioxo-5,9-diazatrideca-3,11-diene; reactivity towards ammonia, 1,2-diaminopropane, hydroxylamine and copper(II) acetylacetonate compounds. Journal of Coordination Chemistry, 2004, 57(6), pp. 509–524. DOI: https://doi.org/10.1080/00958970410001696816
31. Kohtoku, M.; Honma, H.; Takai, O. Electroless plating catalyst performance of a cationic moiety bearing palladium complex. Journal of the Electrochemical Society, 2014, 161(14), pp. D806–D812. DOI: https://doi.org/10.1149/2.0861414jes
32. Geary, W.J. The use of conductivity measurements in organic solvents for the characterisation of coordination compounds. Coordination Chemistry Reviews, 1971, 7(1), pp. 81–122. DOI: https://doi.org/10.1016/S0010-8545(00)80009-0
33. Zhang, X.; Wang, J.; Gao, Y.; Zeng, X.C. Ab initio study of structural and magnetic properties of TM_n(ferrocene)$_{n+1}$ (TM = Sc, Ti, V, Mn) sandwich clusters and nanowires (n = ∞). ACS Nano, 2009, 3(3), pp. 537–545. DOI: https//doi.org/10.1021/nn800794c
34. Montazerozohori, M.; Musavi, S.A.; Naghiha, A.; Veyseh, S. Some new IIB group complexes of an imidazolidine ligand: Synthesis, spectral characterization, electrochemical, thermal and antimicrobial properties. Journal of Chemical Sciences, 2014, 126, pp. 227–238. DOI: https://doi.org/10.1007/s12039-013-0555-y
35. Munyaneza, A.; Kumar, G.; Morobe, I.C. Synthesis, characterization and *in vitro* biological activities of pyrazolylpalladium(II) complexes towards selected strains. Synthesis and Catalysis: Open Access, 2018, 3(1:2), pp. 1–8. DOI: https://doi.org/10.4172/2574-0431.100020
36. Poorabbas, B.; Mardaneh, J.; Rezaei, Z.; Kalani, M.; Pouladfar, G.; Alami, M.H.; Soltani, J.; Shamsi-Zadeh, A.; Abdoli-Oskooi, S.; Saffar, M.J.; Alborzi, A. Nosocomial infections: multicenter surveillance of antimicrobial resistance profile of *Staphylococcus aureus* and Gram negative rods isolated from blood and other sterile body fluids in Iran. Iranian Journal of Microbiology, 2015, 7(3), pp. 127–135. https://www.ncbi.nlm.nih.gov/pmc/articles/PMC4676981/
37. Toval, F.; Köhler, C.D.; Vogel, U.; Wagenlehner, F.; Mellmann, A.; Fruth, A.; Schmidt, M.A.; Karch, H.; Bielaszewska, M.; Dobrindt, U. Characterization of *Escherichia coli* isolates from hospital inpatients or outpatients with urinary tract infection. Journal of Clinical Microbiology, 2014, 52(2), pp. 407–419. DOI: https://doi.org/10.1128/JCM.02069-13
38. Zhang, Q.; Yue, C.; Zhang, Y.; Lü, Y.; Hao, Y.; Miao, Y.; Li, J.; Liu, Z. Six metal-organic frameworks assembled from asymmetric triazole carboxylate ligands: synthesis, crystal structures, photoluminescence properties and antibacterial activities. Inorganica Chimica Acta, 2018, 473, pp. 112–120. DOI: https://doi.org/10.1016/j.ica.2017.12.036
39. EUCAST, European Committee on Antibacterial Susceptibility Testing. Breakpoint tables for interpretation of MICs and zone diameters, version 10.0, 2020. https://eucast.org/clinical_breakpoints/
40. Lambert, P.A. Cellular impermeability and uptake of biocides and antibiotics in Gram-positive bacteria and mycobacteria. Journal of Applied Microbiology, 2002, 92(s1), pp. 46S–54S. DOI: https://doi.org/10.1046/j.1365-2672.92.5s1.7.x
41. Tweedy, B.G. Plant extracts with metal ions as potential antimicrobial agents. Phytopathology, 1964, 55, pp. 910–918. https://apsjournals.apsnet.org/journal/phyto